Universal Bound States of Two Particles in Mixed Dimensions or Near a Mirror

Shina Tan

Phys. Rev. Lett. **109**, 020401 — Published 9 July 2012

DOI: 10.1103/PhysRevLett.109.020401

Universal Bound States of Two Particles in Mixed Dimensions or Near a Mirror

Shina Tan[1]

[1]*School of Physics, Georgia Institute of Technology, Atlanta, Georgia 30332, USA*

Some novel *two*-body effects analogous to the well-known *three*-body Efimov effect are predicted. In the systems considered, particle A is constrained on a *truncated* or *bent* one-dimensional line or two-dimensional plane, or on one side of a flat mirror in three dimensions (3D). The constraining potential is fine-tuned such that particle A's ground state wave function is a constant in the region in which it is constrained. Particle B moves in 3D and interacts with particle A resonantly. An infinite sequence of giant two-body bound states are found in each case.

PACS numbers: 03.75.-b, 21.45.-v, 03.65.Ge, 67.85.-d

Three particles with short range interactions and large scattering length usually have many shallow bound states known as the Efimov states [1–13]. Their sizes greatly exceed the range of the interactions, and they are similar to each other due to a discrete scaling symmetry [1–13]. Initially studied for three particles in three dimensions (3D), Efimov's scenario has been extended to four or more particles in 3D [11, 14–24], to three or four resonantly interacting particles in mixed dimensions - where different particles live in different spatial dimensions [25–28], to five-body systems in one dimension (1D)[29], and to three particles with long-range dipole interactions [30].

All the above effects require *three* or more interacting particles. Although one may have Efimov effect for two particles interacting resonantly with a static point impurity and between themselves, the impurity can be treated as a third "particle", having an infinite mass.

In this Letter we propose some novel scenarios in which one can *not* say a third "particle" (in the normal sense of the word) is involved, and two particles only with *short-range interactions* [31] have many shallow bound states. These two-body states are precisely similar to each other and are universal in the sense that they depend only on such macroscopic parameters as mass ratio and angle, and a single length scale that fixes their overall sizes, but not on any additional microscopic details of the problem.

We propose 7 distinct but related scenarios (skteched in Fig. 1) for two particles A and B, with masses m_A and m_B respectively.

Scenario 1: A is constrained along a half-infinite 1D ray. The ray extends from a fixed point called *vertex*.

Scenario 2: A is constrained along a V-shaped bent line, whose two straight arms form an angle $\theta < \pi$ at a point called *vertex*.

Scenario 3: A is constrained on a half-infinite 2D planar sheet, whose *edge* is a straight line.

Scenario 4: A is constrained on a bent 2D plane, whose two flat sheets form an angle $\theta < \pi$ along a 1D ridge called *edge*.

Scenario 5: A is constrained to one side of a 2D plane (called *mirror*) in 3D space.

Scenarios 6 and 7: A and B are *both* constrained to the same side of a 2D plane (called *mirror*) in 3D space.

In each scenario, the microscopic profile of the constraining potential is not uniquely specified. We only require that the potential be fine-tuned and, in particular, the *depth* of the potential at the vertex, edge, or mirror surface must take some critical value (depending on the microscopic size or thickness of the vertex, edge, or mirror surface), such that the ground state wave function of an *isolated* particle A approaches a finite *constant* away from the vertex, edge, or mirror surface.

In Scenarios 1-5, B does not experience any constraining potential, and can move in the entire 3D space freely. In Scenario 6, the constraining potential for particle B is also fine-tuned such that the ground state wave function of an isolated particle B is a constant on one side of the mirror and zero on the other side. In Scenario 7, the mirror acts as a hard wall for particle B, so that the ground state wave function of an isolated particle B is linearly proportional to its distance from the mirror.

In Scenarios 1 and 2, A and B interact with a 1D-3D mixed dimensional scattering length $a_{\rm eff}$ [25]. In Scenarios 3 and 4, A and B interact with a 2D-3D mixed dimensional scattering length $a_{\rm eff}$ [25]. In Scenarios 5-7, A and B interact with a scattering length a.

In this Letter we show that, if $a_{\rm eff}$ (for Scenarios 1-4) or a (for Scenarios 5-7) is infinite, the two particles have an infinite number of shallow bound states that are similar to each other, and we determine their wave functions *analytically*. The linear sizes of these bound states form a geometric sequence with common ratio

$$\lambda = e^{\pi/s_0} \tag{1}$$

called *scaling factor* (greater than 1), and the binding energies form a geometric sequence with common ratio λ^{-2}, analogous to the Efimov effect [1, 2]. Here s_0 is the positive solution to the transcendental equation

$$F_{s_0}(\alpha) - \cosh(\pi s_0) + \eta(1)\big[1 + F_{s_0}(\pi - \alpha)\big] = 0, \tag{2}$$

where

$$F_{s_0}(\xi) \equiv \frac{\sinh(s_0\xi)}{s_0 \sin\xi}, \tag{3}$$

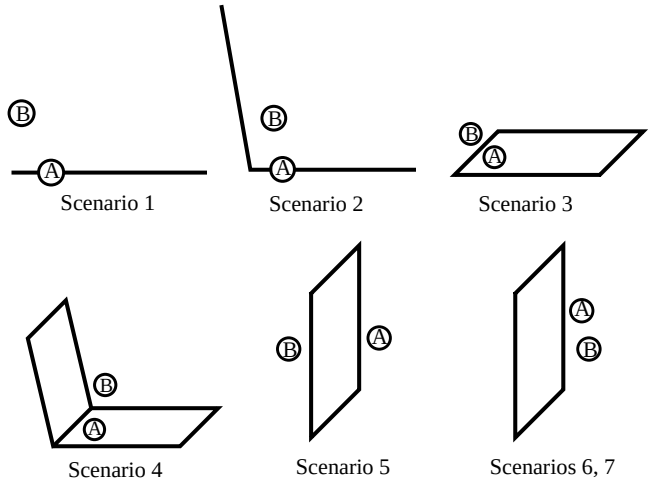

FIG. 1: In Scenarios 1 and 2, particle A is constrained along a 1D ray or bent line. In Scenarios 3 and 4, particle A is constrained on a half-infinite plane or bent plane. In Scenarios 5-7, particle A is constrained to one side of a plane in the 3D space. In Scenarios 1-5, particle B is free to move in the entire 3D space. In Scenarios 6 and 7, particle B is constrained to the same side of the plane as particle A. See text for more details.

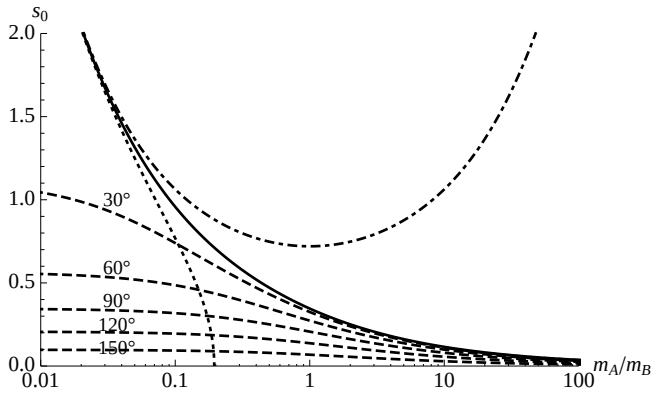

FIG. 2: s_0 versus the mass ratio. The sizes of two adjacent shallow bound states differ by a factor of $\lambda = e^{\pi/s_0}$. Solid line applies to the one-leg vertex effect, one-sheet edge effect, and Type-I mirror effect, as well as the $\theta \to 0$ limits of the two-leg vertex effect and two-sheet edge effect. Dashed lines: two-leg vertex effect and two-sheet edge effect at various values of the angle θ, whose value is labeled on each curve. Dot-dashed line: Type-IIN mirror effect. Dotted line: Type-IID mirror effect (existing at $m_A/m_B < 0.195$ only).

$$\alpha \equiv \begin{cases} \arccos\frac{u-1}{u+1}, & \text{Scenarios 1, 3, 5, 6, and 7,} \\ \arccos\frac{u-\cos\theta}{u+1}, & \text{Scenarios 2 and 4,} \end{cases} \tag{4}$$

$$\eta(1) \equiv \begin{cases} 0, & \text{Scenarios 1-5,} \\ 1, & \text{Scenario 6,} \\ -1, & \text{Scenario 7,} \end{cases} \tag{5}$$

and $u \equiv m_A/m_B$ is the mass ratio.

In Scenarios 1 and 2, the bound pair, or dimer, is pinned near the vertex (although the dimer's size can be arbitrarily large; see above). In Scenarios 3 and 4, the dimer is localized near the edge but can move along the edge freely. In Scenarios 5-7, the dimer is localized near the mirror but can move freely in any direction parallel to the mirror. The emergence of these shallow bound states will thus be called *vertex effects*, *edge effects*, and *mirror effects*, respectively.

The vertex effects in Scenarios 1 and 2 will be called *one-leg vertex effect* and *two-leg vertex effect*, respectively.

The edge effects in Scenarios 3 and 4 will be called *one-sheet edge effect* and *two-sheet edge effect*, respectively.

The mirror effects in Scenarios 5, 6, and 7 will be called *Type-I mirror effect*, *Type-IIN mirror effect* and *Type-IID mirror effect*, respectively. For two resonantly interacting particles near a hard wall with the usual Dirichlet boundary condition, there are no infinite sequence of bound states [32]. The mirror effects predicted in this Letter differ in that at least one particle is subject to the *Neumann* boundary condition instead [see Eq. (21) below].

The values of s_0 for all the seven scenarios are plotted in Fig. 2. Note that in Scenario 7, s_0 vanishes at $u = u_c \approx 0.195$ and there is no real solution for s_0 at $m_A/m_B > u_c$, so the Type-IID mirror effect is limited to $m_A/m_B < u_c$ only. In all the other six scenarios, the infinite sequence of shallow bound states exist for all mass ratios.

We only consider those two-body bound states whose sizes far exceed the range of the interaction; we treat the range as zero and replace the interaction by a Bethe-Peierls (BP) boundary condition [see Eqs. (9), (15) and (23) below]. Equation (2) ensures that the BP condition is satisfied. The two-body binding energies are given by

$$E = -\hbar^2\kappa_n^2/2m_B, \tag{6}$$

where $\kappa_n \equiv \kappa_0\lambda^{-n}$ $(n = 0, 1, 2, \dots)$. The parameter $1/\kappa_0$ is determined by the masses of both particles, the microscopic details of the interaction, and the external potential responsible for the 1D or 2D confinement or the mirror. It plays the same role as the length parameter in the three-body Efimov effect [1, 2].

In the following paragraphs we list the equations satisfied by the low energy states at $|a_{\rm eff}| \to \infty$ (for Scenarios 1-4) or $|a| \to \infty$ (for Scenarios 5-7), and show their bound-state solutions.

In Scenario 1, the two-particle wave function is $\psi = \psi(r_A, \mathbf{r}_B)$, where r_A is the distance of particle A from the vertex, and $\mathbf{r}_B$ is the position vector of particle B relative to the vertex. Since the ground state wave function of an *isolated* particle A is a constant on the ray away from the vertex, ψ satisfies the Neumann boundary condition at low energies (we assume particle A is tightly confined in a quasi-1D geometry, and the two-body energy E relative to the scattering threshold should be much smaller than the microscopic energy scales such as $\hbar^2/2m_A\epsilon^2$, where

$2\pi\hbar$ is Planck's constant, and ϵ is the amplitude of zero-point motion of particle A in the transverse directions):

$$\lim_{r_A\to 0}\frac{\partial\psi}{\partial r_A}=0 \quad \text{when } \mathbf{r}_B\neq 0. \tag{7}$$

ψ also satisfies the Schrödinger equation

$$\Big(-\frac{\hbar^2}{2m_A}\frac{\partial^2}{\partial r_A^2}-\frac{\hbar^2}{2m_B}\nabla_B^2\Big)\psi=E\psi, \quad \mathcal{D}>0 \tag{8}$$

and the BP boundary condition for the 1D-3D mixture with $|a_{\rm eff}|\to\infty$ [25]:

$$\psi\propto 1/\mathcal{D}+O(\mathcal{D}), \quad \mathcal{D}\to 0, \tag{9}$$

where $\mathcal{D}\equiv\big[|\mathbf{r}_B-\mathbf{e}(\mathbf{e}\cdot\mathbf{r}_B)|^2+\frac{u}{u+1}\big(r_A-\mathbf{e}\cdot\mathbf{r}_B\big)^2\big]^{1/2}$ is a measure of the separation between the two particles [25], and $\mathbf{e}$ is the unit vector parallel to the 1D ray along which A is confined. We find a sequence of bound states (labeled by the integer n) with wave functions

$$\psi=\sum_{\sigma=\pm 1}F_{s_0}\Big(\arccos\frac{\sigma u r_A-\mathbf{e}\cdot\mathbf{r}_B}{\sqrt{u+1}\,R}\Big)G_{s_0}(\kappa_n R), \tag{10}$$

where $F_{s_0}(\xi)$ is defined in Eq. (3), $G_{s_0}(y)\equiv y^{-1}K_{is_0}(y)$, $K_{is_0}(y)$ is the modified Bessel function of the second kind which decays exponentially at large y, and $R\equiv(ur_A^2+r_B^2)^{1/2}$. Their energies are given by Eq. (6).

In Scenario 2, let $\psi_\mu(r_A,\mathbf{r}_B)$ be the probability amplitude of finding particle A on the μth arm ($\mu=1$ or 2) of the bent line, at distance $r_A>0$ from the vertex, and particle B at position $\mathbf{r}_B$ relative to the vertex. Since the ground state wave function of an *isolated* particle A is a nonzero constant along the two arms, at low energies $\psi_\mu(r_A,\mathbf{r}_B)$ is a continuous and smooth function of the position of particle A on the bent line:

$$\lim_{r_A\to 0}\psi_1=\lim_{r_A\to 0}\psi_2, \quad \lim_{r_A\to 0}\frac{\partial\psi_1}{\partial r_A}=-\lim_{r_A\to 0}\frac{\partial\psi_2}{\partial r_A}. \tag{11}$$

The Schrödinger equation and the BP boundary condition are given by Eqs. (8) and (9), with ψ replaced by ψ_μ and $\mathcal{D}=\big[|\mathbf{r}_B-\mathbf{e}_\mu(\mathbf{e}_\mu\cdot\mathbf{r}_B)|^2+\frac{u}{u+1}\big(r_A-\mathbf{e}_\mu\cdot\mathbf{r}_B\big)^2\big]^{1/2}$ instead. Here $\mathbf{e}_\mu$ is the unit vector parallel to the μth arm, satisfying $\mathbf{e}_1\cdot\mathbf{e}_2=\cos\theta$. We find a sequence of bound states with wave functions

$$\psi_\mu=\sum_{\nu=1}^{2}F_{s_0}\Big(\arccos\frac{(-1)^{\delta_{\mu\nu}}u r_A-\mathbf{e}_\nu\cdot\mathbf{r}_B}{\sqrt{u+1}\,R}\Big)G_{s_0}(\kappa_n R), \tag{12}$$

where $\delta_{\mu\nu}$ is the Kronecker delta, and $R\equiv(ur_A^2+r_B^2)^{1/2}$. Their energies take the form of Eq. (6).

In Scenario 3, we set up a Cartesian coordinate system whose z axis coincides with the edge of the half-infinite sheet, and whose positive x axis is on the sheet. The wave function is $\psi(x_A,z_A,x_B,y_B,z_B)$, where $(x_A,0,z_A)$ and (x_B,y_B,z_B) are the coordinates of A and B, respectively. ψ satisfies the Neumann boundary condition

$$\lim_{x_A\to 0}\frac{\partial\psi}{\partial x_A}=0 \ \text{ when } x_B^2+y_B^2+(z_A-z_B)^2\neq 0, \tag{13}$$

the Schrödinger equation

$$\Big[-\frac{\hbar^2}{2m_A}\Big(\frac{\partial^2}{\partial x_A^2}+\frac{\partial^2}{\partial z_A^2}\Big)-\frac{\hbar^2}{2m_B}\nabla_B^2\Big]\psi=E\psi, \ \ \mathcal{D}>0 \tag{14}$$

and the BP boundary condition for the 2D-3D mixture with $|a_{\rm eff}|\to\infty$ [25]:

$$\psi\propto\mathcal{D}^{-1}+O(\mathcal{D}), \quad \mathcal{D}\to 0, \tag{15}$$

where $\mathcal{D}\equiv\big\{y_B^2+\frac{u}{u+1}[(x_A-x_B)^2+(z_A-z_B)^2]\big\}^{1/2}$ is a measure of the separation between the two particles [25]. We find a sequence of shallow bound states with wave functions and energies

$$\psi=e^{ik_z z_c}\sum_{\sigma=\pm 1}F_{s_0}\Big(\arccos\frac{\sigma u x_A-x_B}{\sqrt{u+1}\,R}\Big)G_{s_0}(\kappa_n R), \tag{16}$$

$$E=-\hbar^2\kappa_n^2/2m_B+\hbar^2k_z^2/2M, \tag{17}$$

where $z_c\equiv(uz_A+z_B)/(u+1)$ is the z coordinate of the center of mass (C.O.M.), $M\equiv m_A+m_B$ is the total mass, $\hbar k_z$ is the z component of the two particles' total linear momentum, and $R=\big[ux_A^2+x_B^2+y_B^2+\frac{u}{u+1}(z_A-z_B)^2\big]^{1/2}$. The C.O.M. motion in the z direction is decoupled from the remaining degrees of freedom.

In Scenario 4, we set up a Cartesian coordinate system with the edge as the z axis. The two-body wave function is $\psi_\mu(\rho_A,z_A,\mathbf{r}_{B\perp},z_B)$, representing the probability amplitude of finding particle A on the μth ($\mu=1,2$) sheet at distance ρ_A from the edge, with z coordinate z_A, and particle B at position $(\mathbf{r}_{B\perp}+z_B\mathbf{e}_z)$. Here $\mathbf{e}_z$ is the unit vector along the z axis, and $\mathbf{r}_{B\perp}$ is perpendicular to $\mathbf{e}_z$. Let $\mathbf{e}_\mu$ be the unit vector parallel to the μth sheet and perpendicular to the edge: $\mathbf{e}_\mu\cdot\mathbf{e}_z=0$. We have again $\mathbf{e}_1\cdot\mathbf{e}_2=\cos\theta$. The wave function satisfies the continuity and smoothness conditions across the edge

$$\lim_{\rho_A\to 0}\psi_1=\lim_{\rho_A\to 0}\psi_2, \quad \lim_{\rho_A\to 0}\frac{\partial\psi_1}{\partial\rho_A}=-\lim_{\rho_A\to 0}\frac{\partial\psi_2}{\partial\rho_A}, \tag{18}$$

the Schrödinger equation

$$\Big[-\frac{\hbar^2}{2m_A}\Big(\frac{\partial^2}{\partial\rho_A^2}+\frac{\partial^2}{\partial z_A^2}\Big)-\frac{\hbar^2}{2m_B}\nabla_B^2\Big]\psi_\mu=E\psi_\mu, \ \ \mathcal{D}>0 \tag{19}$$

and the BP boundary condition Eq. (15), but now

$$\mathcal{D}=\Big\{\big|\mathbf{r}_{B\perp}-\mathbf{e}_\mu(\mathbf{e}_\mu\cdot\mathbf{r}_{B\perp})\big|^2 + \tfrac{u}{u+1}\big[(\rho_A-\mathbf{e}_\mu\cdot\mathbf{r}_{B\perp})^2+(z_A-z_B)^2\big]\Big\}^{1/2}.$$

We find a sequence of bound states with wave functions

$$\psi_\mu = e^{ik_z z_c} \sum_{\nu=1}^{2} F_{s_0}\Big(\arccos \frac{(-1)^{\delta_{\mu\nu}} u\rho_A - \mathbf{e}_\nu \cdot \mathbf{r}_{B\perp}}{\sqrt{u+1}\, R}\Big) \times G_{s_0}(\kappa_n R), \tag{20}$$

where $R \equiv \big[u\rho_A^2 + r_{B\perp}^2 + \frac{u}{u+1}(z_A - z_B)^2\big]^{1/2}$ and $z_c \equiv (uz_A + z_B)/(u+1)$. The energies of these bound states again take the form of Eq. (17).

In Scenarios 5, 6, and 7, we set up a Cartesian coordinate system whose yz plane coincides with the mirror surface, and whose positive x axis is on the same side of the mirror as particle A. The two-body wave function is $\psi(x_A, y_A, z_A, x_B, y_B, z_B)$, where (x_A, y_A, z_A) and (x_B, y_B, z_B) are the coordinates of particles A and B, respectively. In all three Scenarios, $x_A > 0$. In Scenarios 6 and 7 we also have $x_B > 0$ (but in Scenario 5, x_B may take any value). The wave function satisfies the Neumann boundary condition

$$\lim_{x_A \to 0} \frac{\partial \psi}{\partial x_A} = 0 \ \text{ when } x_B^2 + (y_B - y_A)^2 + (z_B - z_A)^2 \neq 0, \tag{21}$$

the Schrödinger equation

$$\Big(-\frac{\hbar^2}{2m_A}\nabla_A^2 - \frac{\hbar^2}{2m_B}\nabla_B^2\Big)\psi = E\psi, \quad r > 0 \tag{22}$$

and the BP boundary condition with $|a| \to \infty$:

$$\psi \propto r^{-1} + O(r), \quad r \to 0, \tag{23}$$

where $r \equiv \big[(x_A - x_B)^2 + (y_A - y_B)^2 + (z_A - z_B)^2\big]^{1/2}$ is the distance between the two particles. In Scenario 6 the wave function must also satisfy the Neumann boundary condition $\lim_{x_B \to 0} \frac{\partial \psi}{\partial x_B} = 0$ due to a fine-tuning of the mirror potential for particle B at $x_B = 0$, whereas in Scenario 7 it should satisfy the Dirichlet boundary condition $\lim_{x_B \to 0} \psi = 0$ due to a hard wall potential barrier at $x_B = 0$. We find a sequence of bound states with wave functions and energies [33]

$$\psi = e^{ik_y y_c + ik_z z_c} \sum_{\sigma_A = \pm 1} \sum_{\sigma_B = \pm 1} \eta(\sigma_B) \times F_{s_0}\Big(\arccos \frac{\sigma_A u x_A + \sigma_B x_B}{\sqrt{u+1}\, R}\Big) G_{s_0}(\kappa_n R), \tag{24}$$

$$E = -\hbar^2 \kappa_n^2 / 2m_B + \hbar^2(k_y^2 + k_z^2)/2M, \tag{25}$$

where $y_c \equiv (uy_A + y_B)/(u+1)$, $z_c \equiv (uz_A + z_B)/(u+1)$, $R \equiv \big\{ux_A^2 + x_B^2 + \frac{u}{u+1}\big[(y_A - y_B)^2 + (z_A - z_B)^2\big]\big\}^{1/2}$, $\eta(-1) \equiv 1$, and $\eta(1)$ is given by Eq. (5). If particle A is subject to the Neumann boundary condition (21), but particle B is subject to a *mixed* condition $\psi \propto 1 - x_B/a_{1D}^B$ at $x_B \to 0^+$, the two-body spectrum will be type-IID-like for pair sizes $\gg |a_{1D}^B|$, type-IIN-like for pair sizes $\ll |a_{1D}^B|$, and exhibits a smooth crossover in between, analogous to the "Bose-Fermi crossover" in the three-body Efimov spectrum in a 1D-3D mixture [28].

One may realize the scenarios discussed above with ultracold atoms, for which one can use a Feshbach resonance to achieve the two-body BP boundary condition. For Scenarios 1-5, one may apply species-selective optical dipole potentials to constrain the motion of atom A but not atom B [27]. For Scenarios 1-3, the potentials could be produced by some light sources' real images (at the focal plane of a lens or parabolic reflector), superimposed by a 1D optical lattice. To realize the Type-I mirror effect (Scenario 5), one may illuminate the 3D region $x > 0$ with a laser (red-detuned for atom A) whose intensity is deliberately enhanced in a layer of thickness $\sim d$ near $x = 0$, such that atom A's ground state wave function approaches a finite constant at $x \gg d$. To realize the Type-II mirror effects (including Scenarios 6 and 7 but excluding Scenario 5), one may apply a Double Evanescent Wave mirror [34] potential $V(x)$ that is strongly repulsive at $x < \epsilon_1$, attractive at $\epsilon_1 < x \lesssim \epsilon_2$, and negligible at $x \gg \epsilon_2$. At a critical attraction, the ground state wave function of a single atom A approaches a finite constant at $x \gg \epsilon_2$. Then the two-body wave function satisfies Eq. (21) at low energies $|E| \ll \hbar^2/2m_A\epsilon_2^2$.

The Type-IIN mirror effect may be realized with two identical bosons, for which $s_0 = 0.7202$ and the scaling factor $\lambda = 78.4$ [see Eqs. (1) and (2)]. This should be contrasted with the scaling factor 22.7 for the Efimov effect of three identical bosons [1, 2]. (All other two-body effects predicted above require two distinguishable particles.)

To have a denser two-body spectrum, we need a smaller scaling factor λ. This requires a smaller mass ratio m_A/m_B (except for the type-IIN mirror effect where λ is invariant under the interchange of m_A and m_B; see Fig. 2). If one chooses ^{6}Li and ^{133}Cs for A and B respectively, then in the 1-leg vertex effect, 1-sheet edge effect, and type-I mirror effect $\lambda = 9.8$, in the type-IIN mirror effect $\lambda = 9.1$, and in the type-IID mirror effect $\lambda = 10.7$.

For cold atoms, the shallow two-body bound states predicted in this Letter will be free from three-body recombination (if isolated from other atoms and molecules), and can potentially be *much longer lived* than the Efimov trimers created experimentally [3, 5–13].

The spatial mobility of the dimers in Scenarios 3-7 may allow them to be transported and/or manipulated easily.

In summary, we have shown that by tuning two particles near a scattering resonance and delicately constraining the spatial motion of at least one of them, one can create many universal giant two-body bound states. Our scenarios illustrate a close interplay between spatial *geometry* and universal few-body states. For instance, in Scenarios 2 and 4, by merely increasing the *angle* between the two rays or sheets to 180°, one can eliminate the discrete sequence of two-body bound states.

The present work can be extended to large but finite two-body (effective) scattering lengths, or to situations where the external potential for particle A at the vertex, edge, or mirror is slightly detuned such that the particle is subject to a large but finite 1D scattering length in 1, 2, or 3 dimensions. We expect that by reducing the (effective or 1D) scattering length by each factor of λ, one shallow two-body bound state disappears. This is analogous to the three-body Efimov effect (see, eg, Ref. [4]).

By changing the external potentials for particles, one may realize many more types of universal two-body or few-body effects. Here we list just a few examples. **1.** By confining one particle along a thin circle and allowing another to move in 3D, one can produce exotic shallow two-body bound states that are entirely determined by macroscopic parameters such as the mass ratio, the radius of the circle, and the effective scattering length (there is *no* discrete scaling symmetry in this case). **2.** By confining one particle along a hyperbola (a rounded 2-leg vertex) and allowing another to move in 3D, one can produce shallow bound states with discrete scaling symmetry in the infrared limit, with a length parameter $1/\kappa_0$ uniquely determined by the mass ratio and the parameters of the hyperbola. **3.** One can create new types of vertex effects by confining one particle along the arms of an n-leg vertex ($n \geq 3$), which offer many more knobs - the angles between the arms - for controlling the two-body bound states without breaking the discrete scaling symmetry. **4.** In the 1-leg vertex effect, one can drive the excitation or de-excitation of a shallow two-body bound state by placing another 1D ray nearby and injecting a third particle along it. Such universal two-body and few-body effects will be studied in the future.

The author thanks Rudi Grimm, Dean Lee, Yusuke Nishida, and Ran Qi for discussions. This work is supported by the NSF Grant PHY-1068511 and by the Alfred P. Sloan Foundation.

[1] V. Efimov, Phys. Lett. B **33**, 563 (1970).
[2] V. Efimov, Sov. J. Nucl. Phys. **12**, 589 (1971).
[3] T. Kraemer et al., Nature **440**, 315 (2006).
[4] E. Braaten and H.-W. Hammer, Ann. Phys. **322**, 120 (2007).
[5] T. B. Ottenstein et al., Phys. Rev. Lett. **101**, 203202 (2008).
[6] S. Knoop et al., Nature Phys. **5**, 227 (2009).
[7] J. H. Huckans et al., Phys. Rev. Lett. **102**, 165302 (2009).
[8] M. Zaccanti et al., Nature Phys. **5**, 586 (2009).
[9] G. Barontini et al., Phys. Rev. Lett. **103**, 043201 (2009).
[10] N. Gross et al., Phys. Rev. Lett. **103**, 163202 (2009).
[11] S. E. Pollack, D. Dries, and R. G. Hulet, Science **326**, 1683 (2009).
[12] N. Gross et al., Phys. Rev. Lett. **105**, 103203 (2010).
[13] S. Nakajima et al., Phys. Rev. Lett. **106**, 143201 (2011).
[14] G. J. Hanna and D. Blume, Phys. Rev. A **74**, 063604 (2006).
[15] H.-W. Hammer and L. Platter, Eur. Phys. J. A **32**, 113 (2007).
[16] F. Ferlaino et al., Phys. Rev. Lett. **101**, 023201 (2008).
[17] J. von Stecher, J. P. D'Incao, and C. H. Greene, Nature Phys. **5**, 417 (2009).
[18] F. Ferlaino et al., Phys. Rev. Lett. **102**, 140401 (2009).
[19] J. P. D'Incao, J. von Stecher, and C. H. Greene, Phys. Rev. Lett. **103**, 033004 (2009).
[20] F. Ferlaino et al., Laser Phys. **20**, 23 (2010).
[21] J. von Stecher, J. Phys. B: At. Mol. Opt. Phys. **43**, 101002 (2010).
[22] Y. Castin, C. Mora, and L. Pricoupenko, Phys. Rev. Lett. **105**, 223201 (2010).
[23] J. von Stecher, Phys. Rev. Lett. **107**, 200402 (2011).
[24] Y. Wang, W. B. Laing, J. von Stecher, and B. D. Esry, Phys. Rev. Lett. **108**, 073201 (2012).
[25] Y. Nishida and S. Tan, Phys. Rev. Lett. **101**, 170401 (2008).
[26] Y. Nishida and S. Tan, Phys. Rev. A **79**, 060701(R) (2009).
[27] G. Lamporesi et al., Phys. Rev. Lett. **104**, 153202 (2010).
[28] Y. Nishida and S. Tan, Few-Body Syst. **51**, 191 (2011).
[29] Y. Nishida and D. T. Son, Phys. Rev. A **82**, 043606 (2010).
[30] Y. Wang, J. P. D'Incao, and C. H. Greene, Phys. Rev. Lett. **106**, 233201 (2011).
[31] We do not require a spatial dependence [35] of the two-body interaction strength. As Dean Lee pointed out (private communication), if the scattering length has a *linear* spatial dependence, a sequence of two-body bound states with discrete scaling symmetry can emerge. The effects predicted in the present work are very different.
[32] D. Lee and M. Pine, Eur. Phys. J. A **47**, 41 (2011).
[33] In Scenario 6, if the two particles are point-like, be subject to different external potentials, and interact with a symmetric two-body potential, then the binding energies E are symmetric under the *simultaneous* exchange of the masses and the two external potentials, but κ_0 is not, according to Eq. (6). Instead, $\kappa_0/\sqrt{m_B}$ is symmetric.
[34] M. Hammes et al., Phys. Rev. Lett. **90**, 173001 (2003).
[35] R. Qi and H. Zhai, Phys. Rev. Lett. **106**, 163201 (2011).